Study of Sericite Quartz Schist Coarse-Grained Soil by Large-Scale Triaxial Shear Tests

Hui-qing Zhang[1], Feng Zhao[1], Shi-qiang Cheng[1], Yan-qing Zhang[2]*, Ming-jie Gou[2], Hong-jun Jing[2] and Hong-feng Zhi[3]

[1]*Ankang Highway Bureau of Shaanxi Province, Ankang, China,* [2]*School of Architecture and Civil Engineering, Xi'an University of Science and Technology, Xi'an, China,* [3]*Safety Technology Department, Shaanxi Future Energy and Chemical Co. LTD, Yulin, China*

The large-scale triaxial consolidated-drained (CD) and consolidated-undrained (CU) shear tests were carried out to investigate performances of the sericite quartz schist coarse-grained soil on stress-strain, deformation, and strength under four different confining pressure conditions. The test results indicated that the stress-strain curve of sericite quartz schist was nonlinearity, compressive hardening and elastic-plastic. The shear strength envelope curve was better. In the triaxial CD shear test, the sericite quartz schist exhibited weak strain softening under different confining pressures. The sample showed shearing shrinkage at first and later dilatancy under confining pressures of 200, 400, and 600 kPa. When the confining pressure was 800 kPa, the sample showed a trend of shearing shrinkage. In the triaxial CU shear test, the sericite quartz schist exhibited strain hardening, presenting a tendency of shearing shrinkage at first and later dilatancy. It is more reasonable to take account of the cohesion of sericite quartz schist in practical engineering design by linear-regression analysis.

Keywords: soil mechanics, coarse-grained soil, dilatancy effect, characteristics of deformation and strength, large-scale triaxial shear test

HIGHLIGHTS

(1) Large-scale triaxial consolidated-drained and consolidated-undrained shear tests were conducted.
(2) Explored feasibility of coarse aggregates of sericite quartz schist as embankment filler.
(3) Basic engineering mechanical properties of argillaceous limestone were analyzed.

INTRODUCTION

Coarse-grained soil is generally regarded as an earth-rock material with a particle size greater than 0.075 mm and a particle content exceeding 50% of the total mass. Coarse-grained soil is widely distributed in nature. Recently, it was found that coarse sand particles reaching 1 mm size occur on the surface of sand dunes (which have mean particle size 100–300 microns), thereby affecting their shape and dynamics rich in reserves [1]. Coarse-grained soil has excellent engineering performances such as good compaction property, strong water permeability, high shear

strength, and high liquefaction resistance under seismic load. It has been widely used in engineering construction [2]. As the main filler of the roadbed, the performances of the coarse-grained soil have significantly effects on the stability of the construction and the operation of the project. The large-scale triaxial shear tester is an ideal experimental equipment to evaluate the engineering properties of coarse-grained soil. Although it cannot reflect the intermediate principal stress, and the measured value is lower than that of the plane strain gauge and the true triaxial instrument, it is partial to the safety of the engineering application, and it is widely adopted due to the simple principle and operation [3].

Many scholars have conducted in-depth research on the performances of coarse-grained soil. Four groups of large-scale triaxial tests were conducted to investigate the influence of dilatancy on strength and deformation behaviors of coarse-grained soils at different initial densities [4]. Based on large-scale triaxial shearing apparatus, Meng et al. [5] conducted consolidated-drained shear tests on the saturated coarse-grained soil, and put forward a function for fitting the axial strain and lateral strain in the triaxial test, by which the volumetric strain of the soil-sample in the test could be predicted. The triaxial consolidated-drained (CD) shear tests were carried out to examine the stress-strain relationship, strength and deformation property of coarse-grained soil. The influence factors of shear dilatancy coefficient that reflects the degree of dilatancy were explored and the feasibility of the current empirical formulas was verified [6]. Wei et al. [7] experimentally investigated the wetting deformation of a coarse-grained soil at various stress levels, and obtained the relation curve between stress, axial strain, and volume strain. The triaxial tests were carried out to study the development of permeability of crustal rock to help to understand fault mechanics and constrain larger-scale models that predict bulk fluid flow within the crust [8]. In order to study the dilatancy effect of granular soil and its effect on dilatancy tendency under different confining pressure conditions, a series of red stone granular soils tests were executed by the large scale triaxial shearing apparatus [9]. For over coarse-grained soils, the stress-strain relationship, shear strength behavior and the influence of water on strength and deformation under low confining pressures were detailedly analyzed via large-scale triaxial test [10]. Large-scale triaxial shear tests and finite element analysis were carried out to study the deformation properties of coarse-grained soil under static loads [11]. Zhou et al. [12] studied the stress-strain relationship and strength characteristics of the coarse-grained soil in the earthquake area, in which the confining pressure, shear rates, and consolidation time were considered as test variables. The CD triaxial tests were conducted for coarse-grained soil, by means of experiments and particle-based numerical simulations. The numerical model of triaxial test for graded coarse-grained soil was established by programming PFC3D (particle flow code of three dimension) from the view of microscopic scale. Stress-strain relationship from particle flow model and triaxial

test were compared under different confining pressures, and the influence of micro-properties on coarse-grained soil strength was analyzed [13]. A series of large-scale triaxial compression tests was conducted to investigate the effect of stress path on critical state and particle breakage–induced grading evolution of rockfill material [14]. Based on cellular automata method, the HHC-CA model was developed by combining the laboratory triaxial tests of coarse-grained soil, which generated the coarse-grained soil samples of different initial grain fabrics to illustrate the heterogeneous and random distribution of coarse-grained soil grain group. By means of the fast Lagrangian analysis of continua in three dimensions (FLAC3D), triaxial numerical simulation of coarse-grained soil was conducted and the relationship between the gravel content and internal friction angle of sample shear band was discussed [15].

In this paper, the mechanical properties of sericite quartz schist coarse-grained soil under different stress states were investigated. Large size soil samples were adopted to eliminate the size effect of coarse-grained soil and ensure the authenticity of the test results. Large-scale triaxial consolidated-drained (CD) and consolidated-undrained

FIGURE 1 | Large-scale static triaxial apparatus.

TABLE 1 | Indexes of basic properties of samples.

Test material	Specific gravity	Porosity (%)	Water content (%)	Dry density (g/cm^3)
Sericite quartz schist	2.65	18.9	4.6	2.15

(CU) shear tests of coarse-grained soil were carried out at four different confining pressures to evaluate the mechanical properties of coarse-grained soil.

EXPERIMENTAL

Experiment Equipment and Materials

The experiment was conducted on the large-scale static triaxial apparatus (**Figure 1**) of the Nanjing Hydraulic Research Institute (NHRI). The sample size is 300 mm × 700 mm, and the maximum particle size is not exceeding 60 mm.

The test material was the roadbed filler of section K21 + 350-K21 + 541.751 of the second-class road reconstruction project from Xunyang to Ankang, which is part of the national road 316 in shaanxi, China. The lithology of the test material is sericite quartz schist. The indexes of basic properties of samples were listed in **Table 1**, and the gradation curve was shown in **Figure 2**.

Experimental Design

The sample was designed according to the dry density, size and gradation curve of the test. In light of the particle size range, the sample was divided into five equal parts: 60–40 mm, 40–20 mm, 20–10 mm, 10–5 mm, and 5–0 mm. A water permeable plate was placed on the pedestal of the sample, where a rubber membrane was attached on. The forming barrel was installed and the rubber membrane was turned on, then the gas was pumped outside the forming barrel so that the

rubber membrane could be attached tightly to the inner wall of the forming barrel. The first layer of sample was placed, and the surface was flattened evenly. The vibrator was used to make the sample become dense according to the dry bulk density required by each sample. The static pressure of the vibrator plate was 14 kPa, and the vibration frequency was 40 Hz. Then, added the water permeable plate and sample cap on the sample, tightening the rubber membrane, and removed the forming barrel (the triaxial sample after removing the forming barrel was shown in **Figure 3**). Finally, installed the pressure chamber with opened kicker port, and closed the kicker port after filling water into the pressure chamber. The sample was saturated by drip saturation method, and the confining pressure was applied to the saturated sample according to the requirements. The tests could be carried out once the consolidation of the sample was completed.

During the tests, the axial load, axial deformation, displacement and pore water pressure of the sample were
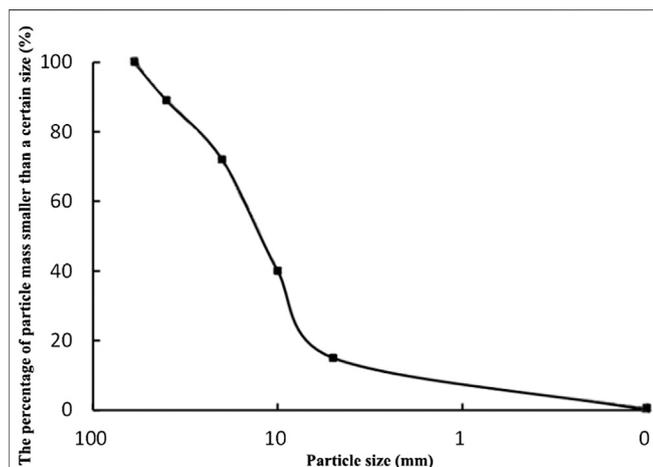
FIGURE 2 | Gradation curve of sericite quartz schist.

FIGURE 3 | Finished sample.

FIGURE 4 | Sample after test.

collected automatically by the computer, and the stress-strain curve was drawn simultaneously until the specimen was broken or the axial strain of the specimen up to 15%.

If there was a failure point, a peak would appear on the stress-strain curve, the value of which represented the principal stress difference ($\sigma_1 - \sigma_3$), corresponding to the failure strength of the rockfill. Otherwise, the point corresponding to 15% of the axial

strain could represent the failure point and the principal stress difference ($\sigma_1 - \sigma_3$) was the failure strength of the rockfill. The above process was repeatedly executed under the confining pressure conditions of 200, 400, 600, and 800 kPa, respectively. The whole test process was carried out according to the Geotechnical Test Procedure (SL237-1999). The sample after the test was shown in **Figure 4**.

RESULTS AND DISCUSSION

Stress-Strain Relationship

The stress-strain relationship curves of CD and CU shear test of samples under different confining pressure conditions were demonstrated in **Figure 5**.

In **Figure 5**, it can be seen that the stress-strain curve of sericite quartz schist exhibited characteristics of nonlinearity, compressive hardening and elastic-plastic. The confining pressure had a significant influence on the stress-strain relationship curve of coarse-grained soil, which was the main effect factor for the strength of the sample. In the initial stage, the initial tangential modulus increased with the increase of confining pressure. When the test condition is constant, the deviatoric stress increased with the increase of confining pressure under the same axial strain condition.

Related researches [16, 17] indicated that grain breakage is smaller under low confining pressure, and increase of grain breakage will significantly degrade material strength. With the increase of particle breakage, the position of the particles is rearranged, and the fine particles fill the voids continuously, so that the sample becomes dense.

For the triaxial CD shear test (**Figure 5A**), the pore water pressure of the sample dissipated rapidly, and under the action of confining pressure, the stress peak occurred when the axial strain is small. However, as the confining pressure increased, the particles were crushed, causing the stress-strain curve of the sample to decrease slightly after reaching the peak stress, and eventually to be residual stress, which was characterized by weak

FIGURE 5 | Stress-strain curves of saturated samples under different confining pressures.

strain softening and mainly due to volume reduction and density increase of the sample.

For the triaxial CU shear test, the volume is constant, and the stress-strain curve had no obvious peak strength, which was characterized by strain hardening. The main reason was attributed to the fracture of coarse particles in the sample, making the sample more dense and not easy to break, so the curve showed a gentle trend.

Deformation Characteristics

Figures 6 and **7** showed the curves of ($\varepsilon_1 \sim \varepsilon_v$) and ($\varepsilon_1 \sim u_w$) of saturated samples under drained and undrained conditions. In this CU shear test, the pore water pressure was measured by the pore pressure sensor at the top of the specimen and was collected automatically by computer.

For the triaxial CD shear test, the volumetric strain of the sample was obtained by measuring the amount of water discharged from the inside of the sample. Under undrained conditions, the sample volume was generally considered to be unchanged. However, for samples with high stone content, due to the sliding extrusion, crushing and filling voids between the stones during the shearing process, the samples also exhibited characteristics of dilatancy and shearing shrinkage [18]. Since the pore water cannot be discharged, the dilatancy and shearing shrinkage tendency of the sample was converted into a constant change of pore water pressure. When the sample showed the dilatancy tendency, the inner pore increased, and the volumetric strain as well as the pore water pressure decreased. When the sample was shearing shrinkage, the inner pore decreased while the volumetric strain and the pore water pressure increased [19].

From **Figures 6** and **7**, it can be found that under drainage condition, when the confining pressures were 200, 400, and 600 kPa, respectively, the volumetric strain increased first and then decreased with the increase of the axial strain, which indicated that the sample was shearing shrinkage at first, then dilatancy later, appearing that the amount of shearing shrinkage increased with the increase of the confining

pressure, then reached the peak, and then the volumetric strain decreased gradually. When the confining pressure was 800 kPa, the sample showed the tendency of shearing shrinkage. The main reason was that the coarse particles in the sample was not be broken under the lower confining pressure, and was easy to turn and roll under the action of shearing force, which was characterized by dilatancy or dilatancy at first, then shearing shrinkage later. According to the discussion in "*Stress-Strain Relationship*" section, the coarse particles in the sample were easily broken under a relatively high confining pressure, and might also be squeezed to fill the pores, rarely flipped and rolled, which was represented as shearing shrinkage macroscopically. For undrained conditions, under the four confining pressure conditions, the overall trend of pore water pressure of the sample was firstly increased and then decreased, indicating that the volumetric strain of the sample increased first and then decreased, showing the tendency of shearing shrinkage at first, then dilatancy later for the sample. When the confining pressure was 200 kPa, the change of pore water pressure of the sample was small and the increase was less than the decrease, indicating that the sample mainly exhibited the dilatancy trend; when the confining pressure is 400, 600, and 800 kPa, the pore water pressure of the sample was larger and the increase is greater than the decrease, indicating that the sample was shearing shrinkage at first, then dilatancy later, and the shearing shrinkage tendency was obvious. In the initial stage, the pore water pressure at a confining pressure of 200 kPa was slightly larger than that under the other three confining pressures, which was related to the compactness of the sample. When the initial pressure was applied, the particles in the sample were mutually displaced and rearranged, resulting in a larger variation of pore volume in the sample, so that the pore water pressure was abrupt. Then the sample was gradually compacted, as the confining pressure increased, the pore water pressure was no longer abrupt, and the curve of pore water pressure became smooth.
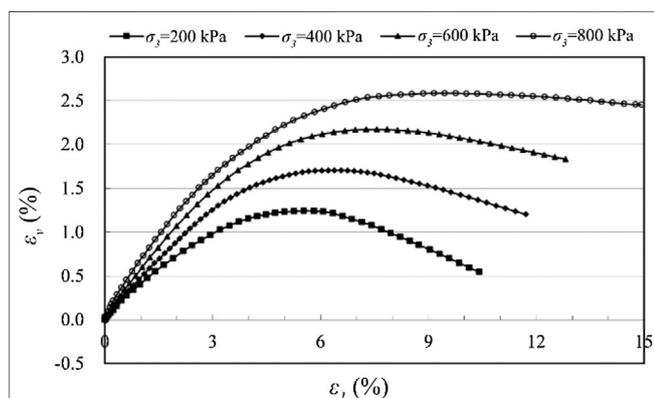
FIGURE 6 | Curves of ($\varepsilon_1 \sim \varepsilon_v$) of saturated sample under different confining pressures (CD).
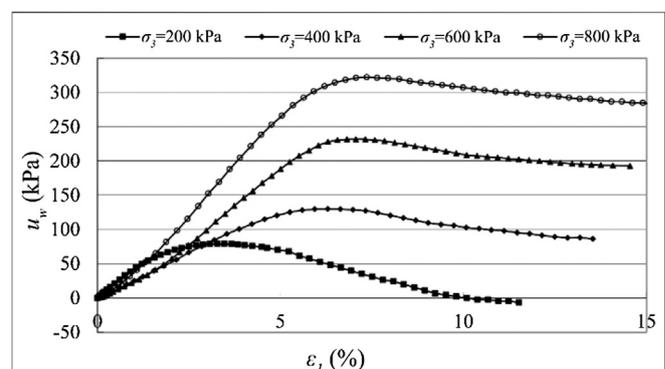
FIGURE 7 | Curves of ($\varepsilon_1 \sim u_w$) of saturated sample under different confining pressures (CU).

FIGURE 8 | Mohr circle and strength envelope of sericite quartz schist (CD).

FIGURE 9 | Total stress strength envelope and effective stress strength envelope of sericite quartz schist (CU).
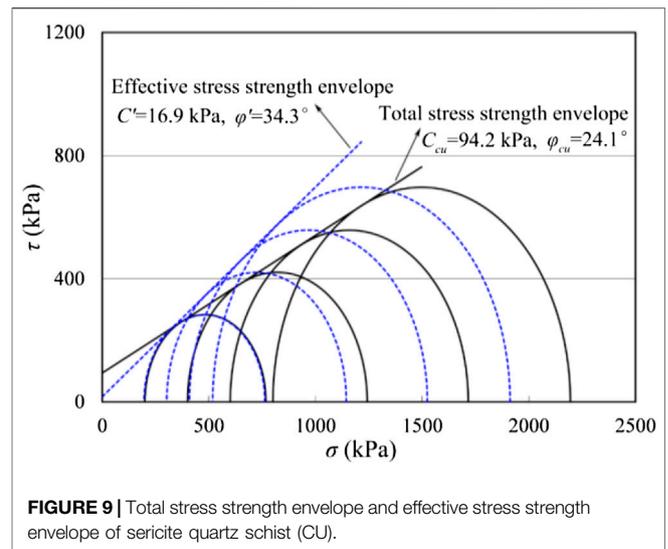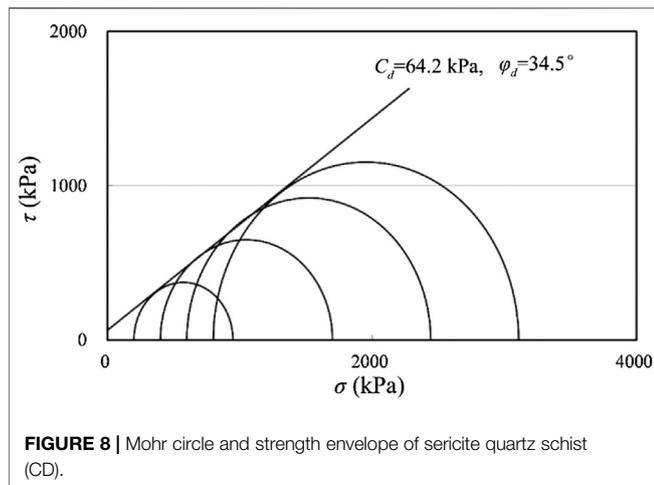
Strength Characteristics

The shear strength of non-cohesive soils mainly comes from the friction and bite force between the soil particles. It is generally recognized that the factors affecting the shear strength of coarse-grained soil include density, coarse particle content, fine particle content, particle geometry, strength of the particles, water content, diameter ratio, sample size and shear speed [20]. For non-cohesive soils, it is generally supposed that the cohesion need not to be considered. However, in the triaxial test, when the Mohr circle strength envelope was fitted by a straight line, there was generally an intercept. The intercept of the non-cohesive soil was related to the bite force between the soil particles, and it is fundamentally different from the cohesion of the cohesive soil. Related tests had shown that the intercept was related to the mineral composition, particle shape, gradation of the soil sample, which was a component of the strength of the granular soil.

There are many different experimental approaches to assess the cohesive properties of polydisperse particle systems, the packing fraction measurement is relatively simple. Parteli et al. [21] applied experiments and numerical simulations to measure the packing fraction of strongly polydisperse powders.

Figures 8 and **9** showed the Mohr circle and the strength envelope of the saturated sample under both drained and undrained conditions.

It can be found that in CD shear test, the internal friction angle (φ) of the saturated sericite quartz schist was 34.5° (**Figure 8**), while in CU shear test, the effective internal friction angle (φ') was 34.3° and the index (φ_{cu}) of total stress strength was 24.1°. The Mohr circle strength envelope was fitted by a straight line, and the cohesion of the roadbed filler was considered in the engineering design. Related research [22] indicated that when the Mohr circle strength envelope was fitted by a straight line, if the cohesion was neglected in the low dam design, the dam was generally conservative; However, if the cohesion was neglected in the high dam design, it was very unreasonable to draw a conclusion that the damage area was obviously larger in the stress-strain calculation.

CONCLUSION

In this study, the CD and CU shear tests of the sericite quartz schist were conducted by using the large-scale triaxial shear apparatus. During the triaxial shearing process, the changes of deviatoric stress, body strain and pore water pressure with the axial strain were monitored comprehensively. The main conclusions are as follows:

1) The large sample well eliminated the size effect of the coarse-grained soil and ensures the reliability of the experimental results. The stress-strain curve of the sericite quartz schist exhibited performances of nonlinearity, compressive hardening and elastic-plastic. Under four confining pressure conditions, the sericite quartz schist showed weak strain softening characteristics in CD shear test and strain hardening characteristics in CU shear test. This was closely related to the volume of the sample and the pore water pressure.

2) The sericite quartz schist presented different dilatancy trends under different confining pressures. For the drained conditions, the samples showed shearing shrinkage at first and dilatancy later under confining pressures of 200, 400, and 600 kPa respectively, while that under 800 kPa just showed shearing shrinkage. For the undrained conditions, the samples showed shearing shrinkage at first and dilatancy later under all the confining pressures.

3) In the CD shear test, the internal friction angle (φ) of saturated sericite quartz schist was 34.5°; In the CU shear test, the effective internal friction angle (φ') was 34.3° and the index (φ_{cu}) of total stress strength was 24.1°. The Mohr circle strength envelope was fitted by a straight line, and the cohesion of the sericite quartz schist was considered in the engineering design to ensure the rationality of the design.

The study results can provide a certain test basis for understanding the engineering characteristics of sericite quartz schist and the stability analysis of rock fill embankment.

DATA AVAILABILITY STATEMENT

All datasets presented in this study are included in the article/supplementary material.

AUTHOR CONTRIBUTIONS

Y-QZ and M-JG, writing-original draft preparation; H-QZ and FZ, methodology; H-JJ and H-FZ, validation; S-QC, supervision. All authors have read and agreed to the published version of the manuscript.

REFERENCES

1. Zhang ZC, Dong ZB, Hu GY, Parteli EJR. Migration and morphology of asymmetric barchans in the central hexi corridor of northwest China. *Geosciences.* (2018). **8**:204. doi:10.3390/geosciences8060204.

2. Guo QG. *Research and application of the engineering properties of coarse-grained soil.* Zhengzhou, China: Yellow River Water Conservancy Press (1998). 12 p.

3. Liu MC, Gao YF, Liu HL, Fei K. Development of study on a large scale triaxial test of coarse-grained materials. *Rock Soil Mech.* (2002). **23**: 217–21. doi:10.1007/s11769-002-0073-1.

4. Jiang JS, Cheng ZL, Zuo YZ, Ding HS. Dilatancy of coarse-grained soil in large-scale triaxial tests study. *Rock Soil Mech.* (2014). **35**:3129–38. doi:10.16285/j.rsm.2014.11.010.

5. Meng F, Zhang JS, Hu QF, Chen XB, Wang QY. Large-scale triaxial test study on volumetric strain law of coarse-grained soil. *Water Resour Hydropower Eng.* (2013). **44**:139–43. doi:10.13928/j.cnki.wrahe.2013.06.034.

6. Chu FY, Zhu JG, Wang GQ, Liu HL. Large scale triaxial test study on deformation and strength characteristics of coarse-grained material. *J Shandong Agric Univ.* (2011). **42**:572–8. doi:10.3969/j.issn.1000-2324.2011.04.021.

7. Wei S, Zhu JG. Study on wetting behavior of coarse grained soil in triaxial test. *Rock Soil Mech.* (2007). **28**:1609–14. doi:10.16285/j.rsm.2007.08.017.

8. Mitchell TM, Faulkner DR. Experimental measurements of permeability evolution during triaxial compression of initially intact crystalline rocks and implications for fluid flow in fault zones. *J Geophys Res.* (2008). **113**:B11412. doi:10.1029/2008jb005588.

9. Chen XB. Study of dilatancy effect of red stone coarse grained soil by large scale triaxial tests. *Chin J Rock Mech Eng.* (2010). **29**:3145–9. doi:CNKI:SUN:YSLX.0.2010-S1-081.

10. Qin SL, Chen SX, Han Z, Xu XC. Large-scale triaxial test study of behavior of over coarse -grained soils. *Rock Soil Mech.* (2010). **31**:189–193. doi:10.16285j.rsm.2010.s2.068.

11. Leng WM, Mei HH, Nie RS, Yang Q, Zhao CY. Static characteristic research on coarse grained soil filling in heavy haul railway subgrade bed. *J Railw Eng Soc.* (2016). **11**:23–9. doi:10.3969/j.issn.1006-2106.2016.11.005.

12. Zhou XJ, Zou Q, Xiang LZ. Mechanical study on the coarse-grained soil using laboratory triaxial shear test. *J Southwest Univ Sci Technol.* (2012). **27**:40–3. doi:10.3969/j.issn.1671-8755.2012.04.009.

13. Geng L, Huang ZQ, Miao Y. Meso-mechanics simulation triaxial test of coarse-grained soil. *J Civ Eng Manag.* (2011). **28**:24–9. doi:10.3969/j.issn.2095-0985.2011.04.006.

14. Ning F, Liu J, Kong X, Zou D. Critical state and grading evolution of rockfill material under different triaxial compression tests. *Int J GeoMech.* (2020). **20**: 04019154. doi:10.1061/(asce)gm.1943-5622.0001550.

15. Wang GJ, Yang CH, Zhang C, Ma HL, Mao HJ, Hou KP. Numerical simulation triaxial tests for coarse-grained soil and preliminary study of initial fabric of sample grain. *Rock Soil Mech.* (2011). **32**:585–90. doi:10.16285/j.rsm.2011.02.047.

16. Hidalgo RC, Herrmann HJ, Partelli EJR. Force chains in granular packings. *Proc Int Sch Phys Enrico Fermi.* (2004). **155**:153–72.

17. Zhang JM, Jiang GS, Wang R. Research on influences of grain breakage and dilatancy on shear strength of calcareous sands. *Rock Soil Mech.* (2009). **30**:2043–8. doi:10.16285/j.rsm.2009.07.056.

18. Chi MJ, Zhao CG, Li XJ. Stress-dilation mechanism of sands. *China Civ Eng J.* (2009). **42**:99–104. doi:CNKI:SUN:TMGC.0.2009-03-022.

19. Xia JG, Hu RL, Qi SW, Gao W, Sui HY. Large-scale triaxial shear testing of soil rock mixtures containing oversized particles. *Chin J Rock Mech Eng.* (2017). **36**:2031–9. doi:10.13722/j.cnki.jrme.2016.1638.

20. Zhang QY, Si HY. Strength and stress-strain properties of the coarse-grained soils by large triaxial shear test. *J Hydraul Eng.* (1982). 22–31.

21. Parteli EJR, Schmidt J, Blümel C, Wirth KE, Peukert W, Pöschel T. Attractive particle interaction forces and packing density of fine glass powders. *Sci Rep.* (2014). **4**:6227. doi:10.1038/srep06227.

22. Gan L, Yuan GG. High pressure large triaxial tests and strength characteristics of coarse-grained soil. *Dam Obs Geotech Tests.* (1997). **21**:9–12. doi:CNKI:SUN:DBGC.0.1997-03-002.